Available online at www.sciencedirect.com
ScienceDirect
Ceramics International 34 (2008) 639–643
CERAMICS INTERNATIONAL
www.elsevier.com/locate/ceramint

Morphology investigation of mechanically activated $ZnO–SnO_2$ system

T. Ivetić [a,*], Z. Vuković [b], M.V. Nikolić [c], V.B. Pavlović [a], J.R. Nikolić [d], D. Minić [e], M.M. Ristić [f]

[a] *Institute of Technical Sciences of SASA, Knez Mihailova 35, 11000 Belgrade, Serbia*
[b] *Institute of Chemistry, Technology and Metallurgy, Department of Catalysis and Chemical Engineering, Sector of Catalysis, Njegoševa 12, 11000 Belgrade, Serbia*
[c] *Center for Multidisciplinary Studies of the University of Belgrade, Kneza Višeslava 1, 11000 Belgrade, Serbia*
[d] *Faculty of Physics, University of Belgrade, Studentski trg 12, 11000 Belgrade, Serbia*
[e] *Faculty of Physical Chemistry, University of Belgrade, Studentski trg 12-16, 11000 Belgrade, Serbia*
[f] *Serbian Academy of Science and Arts, Knez Mihailova 35, 11000 Belgrade, Serbia*

Received 14 November 2006; received in revised form 6 December 2006; accepted 17 January 2007
Available online 6 March 2007

Abstract

Powder mixtures of zinc oxide and tin oxide in the molar ratio, $ZnO:SnO_2 = 2:1$, were mechanically activated in a planetary ball mill in the time intervals of 0–160 min. The adsorption–desorption isotherms, specific surface area, pore volume and pore size distribution spectra of mechanically activated powder mixtures were established by N_2 adsorption at 77 K. Microstructure analysis was performed using scanning electron microscopy (SEM) and digital pattern recognition (DPR) microstructure quantity analysis. The phase composition of the mixed powders was determined by X-ray analysis. Mechanochemical activation of the $ZnO–SnO_2$ system resulted in fine grinding of the starting particles and generation of contacts between them, mass transfer at contacts zones and formation of Zn_2SnO_4 spinel, which was observed after 40 min of activation.

Keywords: A. Milling; A. Powders: solid-state reaction; D. Spinels; Microstructure analysis

1. Introduction

It is well known that materials based on the $ZnO–SnO_2$ system are widely used for the production of humidity and combustible gas detection sensors, coatings for the use in photoelectrochemisty and for fabrication of electrical contacts [1–4]. Since the wide range of applications of these materials is markedly influenced by the morphology of the initial powders it is very important to control the morphology, texture and particle size distribution during the powder preparation process. In order to obtain spinel Zn_2SnO_4 various processing routes, including the conventional high temperature solid-state reaction between ZnO and SnO_2, spray pyrolysis, sol–gel and coprecipitation method have been proposed [5–7]. The mechanochemical processing route has been developed recently for the production of many nano-sized oxides including some with a perovskite and spinel structure. The advantage of this process is that the chemical reactivity of starting materials can be significantly improved during mechanochemical activation, so the solid-state reaction could be activated only due to mechanical energy instead of high temperatures. Furthermore, as a result of physical–chemical changes in the material, which occur as a result of mechanochemical activation, these powders possess much higher sinterability than those synthesized by a conventional solid-state reaction and with most wet chemical processes. Mechanical activation by grinding is a collection of processes that mostly emerge in four stages: material destruction, formation of a new surface on the material which is destroyed, fine grinding and transformation into a new material with a completely different structure [8]. Finding the optimal conditions in the first stage of powder processing—preparation of powders (in this case grinding) gives the opportunity of shortening the sintering time needed for complete formation of the desired compound [9]. Having all this in mind, in this article we investigated the influence of mechanochemical activation

* Corresponding author. Tel.: +381 11 637 367; fax: +381 11 185 263.
E-mail address: tamara@itn.sanu.ac.yu (T. Ivetić).

0272-8842/$34.00
doi:10.1016/j.ceramint.2007.01.003

on the ZnO–SnO_2 system, its effect on the microstructure and development of extensive regions of Zn_2SnO_4 spinel.

2. Experimental

Mixtures of zinc oxide (99.9%, Aldrich) and tin oxide (99.9%, Aldrich) powders, molar ratio ZnO:SnO_2 = 2:1, were mechanically activated in a planetary ball mill (Fritsch Pulverisette 5) in the continuous grinding process regime, in air, and for 10–160 min. We used zirconium oxide grinding balls (10 mm in diameter, approximately) and bowls (500 cm^3) with a ball to powder mass ratio of 40:1. Different milled powder mixtures were denoted according to the applied time of activation as ZSO-10, ZSO-40, ZSO-80 and ZSO-160. The non-activated powder mixture containing ZnO and SnO_2 was marked as ZSO-00.

Phase analysis was carried out in an X-ray diffractometer (Norelco-Philips PW-1050) with Cu Kα radiation at a scanning speed of 0.02°/0.4 s.

Nitrogen adsorption isotherms of mixed powders were determined on a Sorptomatic 1990 adsorption analyzer (Thermo Finnigan) at −196 °C. All samples were degassed at 300 °C for 24 h prior to the measurements. Various models and appropriate software—WinADP were used to analyze the obtained isotherms. The change of specific surface area, S_{BET}, during mechanical activation was calculated according to the Brunauer, Emmett, Teller (BET) method (Table 1) from the linear part of the nitrogen adsorption isotherms ($0.05 < p/p_0 < 0.35$) [10–12]. The pore size distribution for mesopores was calculated in the radius range from 0 to 100 nm by the Dollimore–Heal Poresizes method from the desorption branch of isotherm [13] while micropore volume was determined from the Dubinin Radushkevich Line method [14]. The morphology of obtained powders was characterized using scanning electron microscopy (JEOL JSM-646OLV) and digital pattern recognition (DPR) microstructure quantity analysis [15] that was performed for the obtained SEM micrographs. This method is based on extraction of the foreground layer of a micrograph, its grayscale segmentation, extraction of contours of the segmented object and FFT analysis of the angular distribution of contour radii. It should be mentioned that the relative estimated error of volume diameter distribution calculated by this method is less than 5% for micrographs of very complex systems [16].

3. Results and discussion

Mechanochemical synthesis is a heterogeneous solid-phase reaction in which dispersion of the components, generation of contacts between them and mass transfer at contact zones occurs. As a result of grinding of initial components, change of the powder morphology, their distribution, interface interaction, as well as the change of specific surface area may appear. Specific surface area distribution analysis showed that during grinding of the ZnO–SnO_2 system, two stages emerge (Fig. 1). During the first one, an increase of the specific surface area (S_{BET}) from 6.47 to 8.29 m^2/g is observed, while during the second one, the decrease of the S_{BET} from 8.29 to 2.74 m^2/g. The increase of the S_{BET} during the first stage of ZnO–SnO_2 grinding may be related to breaking of powder particles and formation of a new surface, while cold-welding of the initial powder mixture, which arises in the second stage of grinding, may lead to mechanochemical reactions in the system, formation of new phases and decrease of the S_{BET}. These conclusions are in accordance with the results obtained by XRD analysis (Fig. 2). The initial powder mixture exhibits sharp peaks of hexagonal ZnO (JCPDS PDF 36-1451) and tetragonal SnO_2 (JCPDS PDF 41-1445), while after 10 min of mechanical treatment intensities of all starting phases were significantly lowered. Lowering and broadening of diffraction peaks indicates significant refinement in crystallite size and defect formation during the initial stage of mechanochemical activation. Calculations of the values of mean crystallite size and the relative lattice strain obtained from the diffraction line broadening of the non-activated samples and the samples activated for 10 min pointed out that the mean crystallite size of SnO_2 and ZnO phase decreased from 76 to 65 nm and from 93 to 17 nm, respectively, while the relative lattice strain of these phases increased from 0.126 to 0.148 and from 0.076 to 0.428,

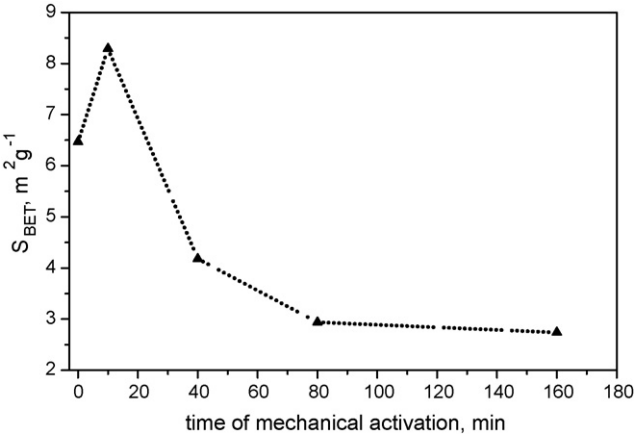

Fig. 1. Change of the specific surface area in the range of 0–160 min of activation.

Table 1
Porous property of non-milled and milled ZnO–SnO_2 powder mixtures

Sample	S_{BET} (m^2/g)	$V_{0.99}$ (cm^3/g)	$V_{micropore}$ (cm^3/g)	D_{median} (nm)	$V_{cumulative}$ (cm^3/g)
ZSO-00	6.47	0.026	0.0019	26.439	0.0402
ZSO-10	8.29	0.034	0.0031	22.552	0.0458
ZSO-40	4.18	0.029	0.0014	52.175	0.0386
ZSO-80	2.94	0.02	0.0012	79.140	0.0247
ZSO-160	2.74	0.02	0.0011	67.497	0.0253

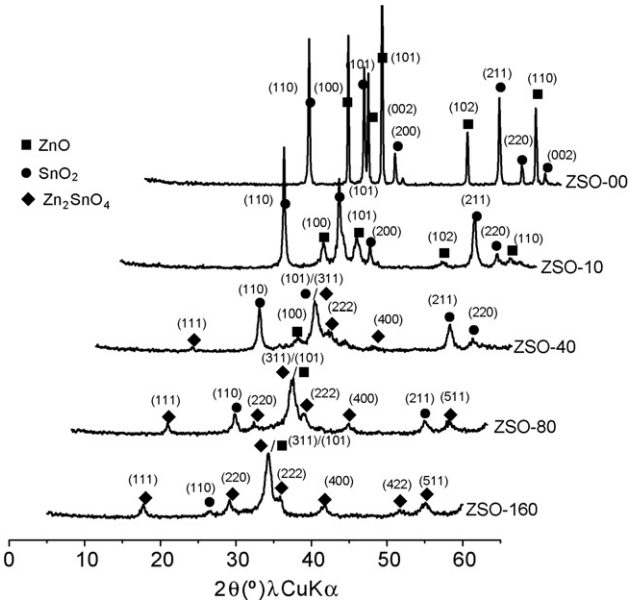

Fig. 2. XRD patterns of ZSO powder mixtures as a function of the time of activation.

respectively. In agreement with microstructure analysis, in the early stages of activation, continuous shearing across interfaces of ZnO and SnO_2 resulted in an increase of their interface area and intermixing of the two components (Fig. 3). As the activation time increased up to 40 min appearance of the spinel zinc stannate phase (Zn_2SnO_4) besides the ZnO and SnO_2 phases was noticed, thus indicating the beginning of mechanochemical reactions in the system. With the increase of the activation time the intensities of ZnO and SnO_2 peaks become lower, while the Zn_2SnO_4 peaks become higher. Calculations of the values of the mean crystallite size and the relative lattice strain of Zn_2SnO_4 for the samples activated 80 and 160 min pointed out an increase of the mean crystallite size of Zn_2SnO_4 from 14 to 29 nm as the activation time increased, while the relative lattice strain decreased from 0.520 to 0.260. Constant collisions and rearrangement of the powder particles provided by mechanical impact, shock, shear, and deformation created opportunities for two or more Zn_2SnO_4 nuclei to meet at favorable positions leading to growth in crystallite size. Thus, the growth of nanocrystallites is a result of constant collisions and rearrangement of the nanocrystalline nuclei proceeding as the activation time increased. After 160 min of mechanochemical activation zinc stannate as a major phase, with insignificant amounts of unreacted ZnO and SnO_2, was observed.

It should be noticed that, simultaneously with the formation of the new Zn_2SnO_4 phase, secondary agglomeration occurred as well, resulting in a continuous decrease of S_{BET} during the second stage of ZnO–SnO_2 system grinding. This observation, as well as the ones obtained by microstructure analysis of the influence of the mechanochemical activation on powder morphology evolution—SEM (Fig. 3), is also in accordance with the results obtained by the XRD analysis.

In the case of non-activated samples we noticed that the initial mixture consisted of two homogeneously distributed particles types: smaller ones, with a spherical shape and

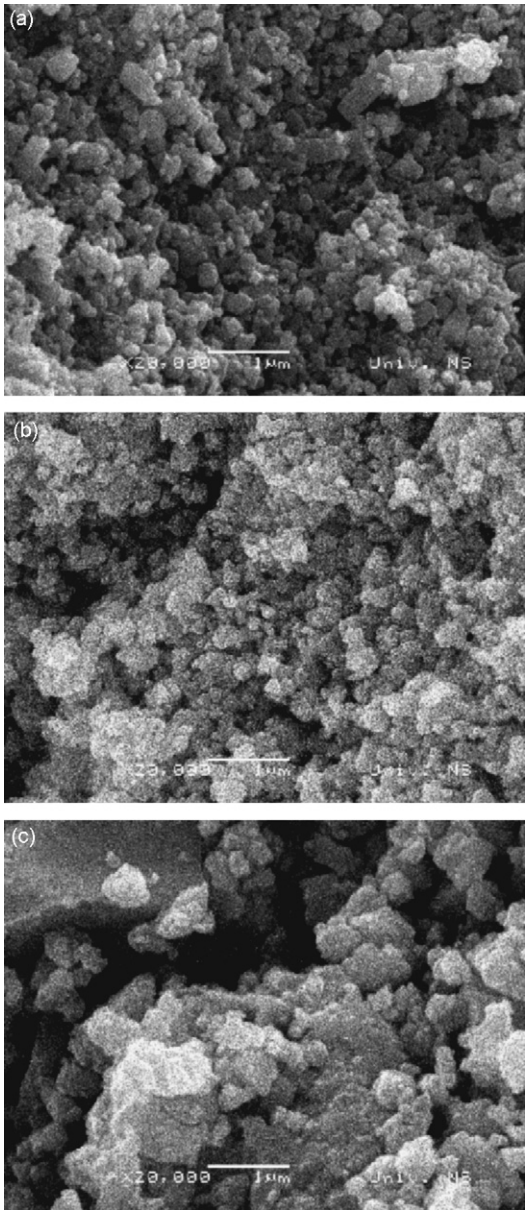

Fig. 3. SEM micrographs of samples: (a) ZSO-00; (b) ZSO-10; (c) ZSO-160.

average size of 0.15 μm, which belong to ZnO and longer ones, with a polygonal shape and average size of 0.25 μm, which belong to SnO_2 (Fig. 4). Activation longer than 10 min brings about an increase in the specific surface area and chopping of particles especially those with a spherical shape. The dominant decrease in the number of spherical particles, after 10 min of activation, appears primarily because they belong to the ZnO phase that is a more than six times softer material than tin oxide (microhardness values are 1.5 and 10 GPa for ZnO and SnO_2, respectively). For the samples activated 160 min, according to histograms obtained by DPR analysis (Fig. 4C) four peaks at 0.15, 0.3, 0.7 and 1.2 μm were noticed. They were ascribed to the average grain size of ZnO, SnO_2 and Zn_2SnO_4 phase and agglomerates, respectively.

Fragmentation and aggregation of particles, occurring during mechanochemical synthesis, have also been observed

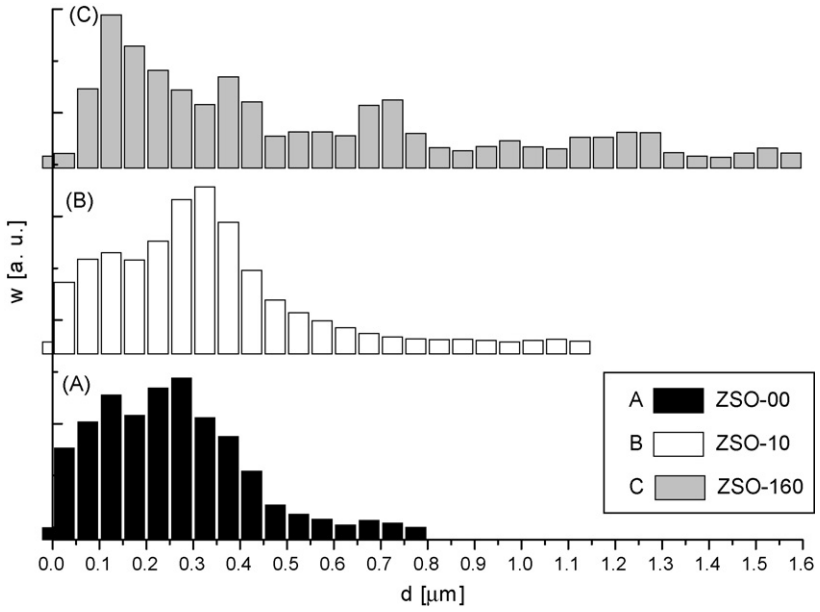

Fig. 4. Digital pattern recognition (DPR) histograms for ZSO-00; ZSO-10; ZSO-160.

from the shape of the adsorption isotherms (Fig. 5). We have noticed that all adsorption isotherms, according to the IUPAC [12,17] classification belong to the Type IIb, which is commonly related to mono-multi layered adsorptions on a clear and stable powder surface, which may exhibit fractured particles, aggregates and macro pores or even in limited micro pores. All isotherms have a reversible part at low relative pressures and hysteresis loops at higher relative pressures which is characteristic of aggregates plane particles in forming slit shape pores [11,12]. Namely, physical adsorption is in most cases reverse. With isothermal decrease in pressure desorption is happening along the same isotherm. However, in very porous adsorbents inside fine pores and capillaries condensation can occur on lower pressures than the equilibrium pressure. Desorption is then harder and the adsorption curve shows a hysteresis during desorption [18]. Our analysis showed that pores with the biggest total bulk volume were determined in the samples activated for 10 min. Decrease of the pore bulk condition decreases the total pore volume. A lower total porosity (volume) was observed in samples activated 80 and 160 min (0.025 ± 0.003 cm^3/g) versus other sample porosity. Mean mesopore diameters, according to the Dollimore–Heal method, vary from 22 nm for samples activated 10 min to 79 nm for the samples activated 80 min. The volume share of the biggest pores (mesopores) decreased for higher activation times so samples activated for 80 and 160 min had smaller amount of the big pores. The increase of the activation time did not lead to further texture development and porosity improvement. Figs. 5 and 6 shows the adsorption–desorption isotherms and pore size distribution spectra (PSD) of the analyzed powder mixtures. Textural properties obtained from N_2 isotherms, PSD curves and by Dubinin–Radushkevich method are summarized in Table 1.

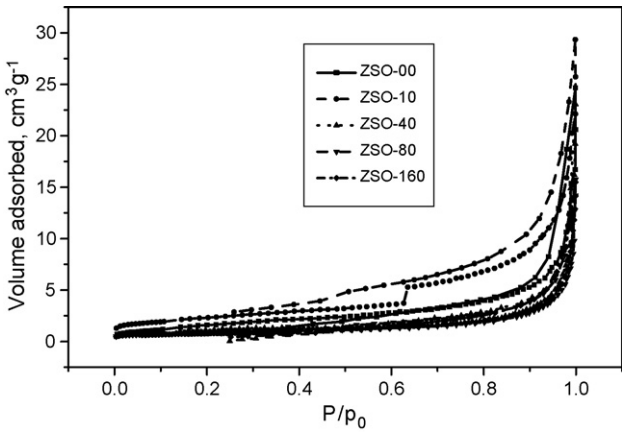

Fig. 5. Nitrogen adsorption–desorption isotherms of different activated powder mixtures.

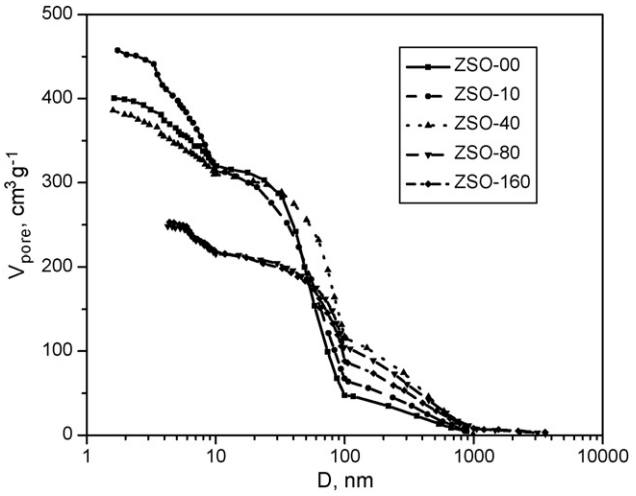

Fig. 6. Pore size distribution (PSD) spectra of different activated powder mixtures.

4. Conclusion

In this article the influence of mechanochemical activation on the ZnO–SnO_2 system has been investigated. Mechanical activation in the observed ZnO–SnO_2 system resulted in fine grinding of the starting particles and generation of contacts between them, mass transfer at the contact zones and synthesis of Zn_2SnO_4 spinel, which was observed after 40 min of activation. XRD and specific surface area distribution analysis pointed out that during mechanical activation of the ZnO–SnO_2 system two processes emerged. The first one was related to breaking of the powder particles and formation of a new surface while the second one led to mechanochemical reactions in the system and formation of a new phase. Fragmentation and aggregation of the particles, which occur as a result of mechanochemical synthesis, has been investigated by SEM, DPR and pore morphology evolution from adsorption isotherm analysis. As a result of this analysis it is possible to optimize the best conditions of powder preparation prior to the sintering process as well as to optimize the processing route for the advanced mechanochemical synthesis of zinc-stanate spinel.

Acknowledgement

This work was performed as part of project 142011G financed by the Ministry for Science and Environmental Protection of the Republic of Serbia.

References

[1] W.J. Moon, J.H. Yu, G.M. Choi, The CO and H_2 gas selectivity of CuO-doped SnO_2–ZnO composite gas sensor, Sens. Actuators B 87 (2002) 464–470.
[2] J.H. Yu, G.M. Choi, Selective CO gas detection of Zn_2SnO_4 gas sensor, J. Electroceram. 8 (2002) 249–255.
[3] D.E. Scaife, Oxide semiconductors in photoelectrochemical conversion of solar energy, Solar Energy 25 (1980) 41–54.
[4] J.H. Yu, G.M. Choi, Current–voltage characteristics and selective CO detection of Zn_2SnO_4 and ZnO/Zn_2SnO_4, SnO_2/Zn_2SnO_4 layered-type sensors, Sens. Actuators B: Chem. 72 (2001) 141–148.
[5] I. Stambolova, K. Konstantinov, D. Kovacheva, P. Peshev, T. Donchev, Spray pyrolysis preparation and humidity sensing characteristics of spinel zinc stannate thin films, J. Solid State Chem. 128 (1997) 305–309.
[6] X. Wu, T.J. Coutts, W.P. Mulligan, Properties of transparent conducting oxides formed from CdO and ZnO alloyed with SnO_2 and In_2O_3, J. Vac. Sci. Technol. A: Vac. Surf. Films 15 (1997) 1057–1062.
[7] G. Fu, H. Chen, Z. Chen, J. Zhang, H. Kohler, Humidity sensitive characteristics of Zn_2SnO_4–$LiZnVO_4$ thick films prepared by the sol–gel method, Sens. Actuators B: Chem. 81 (2002) 308–312.
[8] M.M. Ristic, S.Đ. Milosevic, Mechanical Activation of Inorganic Materials, Serbian Academy of Sciences and Arts, Belgrade, 1998.
[9] N. Nikolic, T. Sreckovic, M.M. Ristic, The influence of mechanical activation on zinc stannate spinel formation, J. Eur. Ceram. Soc. 21 (2001) 2071–2074.
[10] P. Nortier, P. Fourre, A.B. Mohammed Saad, O. Saur, J.C. Lavalley, Effects of crystallinity and morphology on the surface properties of alumina, Appl. Catal. 61 (1990) 141–160.
[11] S.H. Gregg, K.S. Sing, Adsorption, Surface Area and Porosity, Academic Press, New York, 1967.
[12] F. Rouquerol, J. Rouquerol, K. Sing, Adsorption by Powders and Porous Solids, Academic Press, London, 1999.
[13] D. Dollimore, G.R. Heal, An improved method for the calculation of pore size distribution from adsorption data, J. Appl. Chem. 14 (1964) 109–114.
[14] M.M. Dubinin, Physical adsorption of gases and vapors in microspores, in: D.A. Cadenhead (Ed.), Progress in Surface and Membrane Science, vol. 9, Academic Press, New York, 1975, pp. 1–70.
[15] Z.M. Nikolić, V.B. Pavlović, DPR analysis of microstructural evolution of ZnO ceramics, Mater. Sci. Forum 453/454 (2004) 453–457.
[16] V. Pavlović, D. Petrović, Z. Nikolić, V.B. Pavlović, Automatic microstructure analysis of sintered materials, FME Trans. 34 (2006) 159–163.
[17] K.S.W. Sing, D.H. Everett, R.A.W. Haul, L. Moscou, R.A. Pierotti, J. Rouguero, T. Siemieniewska, Reporting physisortion properties data for gas/solid systems with special reference to the determination of surface area and porosity, Pure Appl. Chem. 57 (1985) 603–619.
[18] T. Ivetic, M.Sc. Thesis, Belgrade, 2006 (in Serbian).